

10. TOWARDS RESILIENT OFFSHORE WIND FARMS

David Wilkie¹ and Carmine Galasso¹

¹ University College London, Department of Civil Environmental and Geomatic Engineering., Chadwick Building, Gower Street, London, WC1E 6BT

ABSTRACT. This paper proposes using a performance-based engineering (PBE) approach to quantify the reliability of offshore wind turbines (OWT), for use in a larger assessment of wind farm resilience. The concept of resilience provides a useful framework for considering an OWT as a system that is comprised of both structural and mechanical components and to extrapolate these risks across a farm. An implementation based on the financial consequence of failure is used here, this allows failure states to be defined that combine analytical structural failure scenarios with empirical mechanical equipment failure rates within a unified calculation of material losses. The loss associated with the failure of each component is used to estimate the total annual loss for a case study farm. Results are presented in the form of a case study and indicate that failure of the structure may have an impact on the overall failure profile of the farm. This method provides a simple estimate of robustness for the farm, which is a component of any resilience assessment. It also provides a foundation from which a more detailed assessment of resilience, including adaptability and recovery, will be developed.

Keywords: Offshore Wind, Structural Reliability, Resilience Framework, Loss Modelling, Site Assessment.

1. INTRODUCTION

The offshore wind industry has grown to the point where it supplies 11.03GW [1] of electricity within Europe [1], with a further 26.4GW worth of projects approved [2]. Within European waters most existing OWTs are supported on monopile foundations [3]; these are effectively large diameter cylinders that are hammered into the seabed; on top of which is fixed a rotor and tower, a tapered tubular member connecting the monopile to the rotor. However, the overall cost of offshore wind farms (OWF) remains high and a recent UK government report [4] has highlighted “integrated design” as an area that could improve cost reduction. This aim is challenging as OWTs are unique civil engineering structures in that they rely on both mechanical components (such as a generator, gearbox and control system) and structural components (the tower and monopile) in order to remain operational. Additionally, structural design of OWT is undertaken at the component level, with the tower and monopile commonly being designed by separate companies [5]. Prescriptive codes [6], [7] are used to evaluate potential designs but these do not explicitly consider (i.e., through a full probabilistic approach to analysis and design) the risk posed by uncertainties associated with variability in physical properties nor all of the highly variable natural hazards to which OWF are exposed. Safety factors are instead used to achieve a target (structural) reliability level at both component and system level. Any integrated assessment should account for the above uncertainties in an

explicit manner, also considering the possible complex interrelations between components; for example, stopping the rotor will change loading on the blades, which will in turn influence loads on the tower and monopile. The problem lies in quantifying the risk posed by these diverse sub-systems and accounting for the impact of failures on the overall operability of the farm.

The concept of resilience provides a framework to consider this problem. It has been used within a large number of fields ranging from design to preparedness of communities exposed to environmental hazards [8] and when applied to structural systems [9] incorporates: robustness, redundancy, rapidity and resourcefulness. These represent the ability of a structure to withstand an extreme event and the time required to re-instate operability afterwards, as indicated on Figure 1. However, the properties are difficult to quantify especially from the perspective of a design stage study, where information regarding the capacity of an organisation to make budget available (i.e. resourcefulness) is unlikely to be available to the design engineer. Therefore, a technique for estimating resilience that only relies on the robustness and redundancy of the structure would allow the concept to be applied at the design stage. The initial design estimate of robustness could be used in a later resilience calculation by the asset operator, which also considers resourcefulness. One approach, investigated by Bruneau and Reinhorn [10], assumes that loss of functionality after an extreme event and the time to recovery are correlated. This is intuitive, as in the general case if an event (i.e. wind storm) causes more damage it will take longer to repair structures as a result. This assumption provides a starting point for considering resilience of OWF and has previously been applied to PBE of structures for blast [11] by defining a relative resilience indicator (RRI), which is correlated to resilience (R):

$$R(E) \propto RRI(E) = 1/C(E) \quad (1)$$

Where RRI can be defined as the inverse of the consequence (C) of an extreme event (E). Under this assumption a structure that experiences a lower consequence (i.e. less damage) as the result of a hazard is viewed as more resilient.

The measure of consequence needs to efficiently capture the impact of failure on the system. An OWT is a system comprised of structural and mechanical components, therefore some typical structural consequence measures are not applicable, such as percentage of the structure collapsing [11]. In this study we relate the consequence of failure to the financial impact of a system failure and specifically material loss incurred by failure. This allows the severity of different sub-systems to be compared by using a single measure which is easy to communicate to different stakeholders but neglects the operational costs of repair, such as hiring vessels, which are expensive but difficult to quantify. Metrics relating to life safety are not of primary importance as the wind turbine is normally unmanned, apart from brief periods for maintenance.

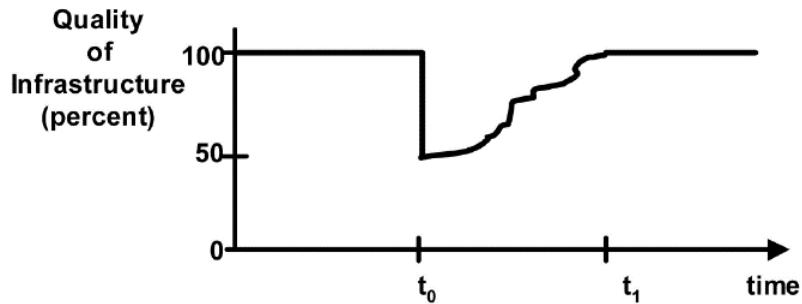


FIGURE 1. Graphical definition of resilience after an event (at t_0).
Adapted from: Brunneau et al [8].

A consequence metric based on component material cost requires a probabilistic model describing the likelihood of incurring these losses. The analytical method we apply to model combined losses of structural and mechanical components is discussed in Section 2. This includes a procedure for evaluating failure probability of the structure based on a PBE technique, which employs dynamic structural analysis. The overall calculation is illustrated through a case-study where a farm NREL 5MW OWT has been assessed at a real wind farm site. Section 3 introduces the case study site and describes the structural reliability calculation. While Section 4 demonstrates the loss calculation for the combined OWT system.

2. LOSS FRAMEWORK

Loss calculation for an OWT system requires both: information concerning costs of failure and the failure frequencies for all relevant components. In this work we focus on severe failure associated with major repairs or component replacement, and not on routine maintenance or loss of production. Failure of the equipment is relatively common and databases of empirical failure rates exist [12]. However, structural components fail less frequently, and they are designed specifically for each wind farm [5], therefore a site-specific approach is necessary to define average failure rates. This section summarises an approach for calculation structural failures and how these are used in a calculation of system loss.

2.1 Structural Reliability

A framework for calculating the probability of incurring different levels of loss arising from failure of an OWT structure has been developed previously by the authors [13]. This considers failure in the turbine's ultimate limit state, i.e., the turbine locally collapsing during storm conditions. A brief overview of the background to the approach is presented here, full details are available in the reference.

The approach is based on PBE which was originally proposed by the Pacific Earthquake Engineering Research (PEER) centre to assess failure of structures due to seismic hazards [14], and the approach has subsequently been expanded to consider a range of hazards including wind [15], [16] and blast [11]. It is based on downgrading risk into conditional distributions that are evaluated sequentially using total probability theorem. This approach can

express consequence as expected material loss ($E(L)$) in terms of conditional probability density functions ($f(\cdot | \cdot)$):

$$E(L) = \int \int \int E[L|DM] \cdot f[DM|EDP] \cdot f[EDP|IM] \cdot f(IM) \cdot dDM \cdot dEDP \cdot dIM \quad (2)$$

Where the terms are damage measure (or DM), a parameter describing structural response (engineering demand parameter, or EDP) e.g. a force or stress, and the intensity of a natural hazard (intensity measure, or IM) e.g. wind speed or wave height. This framework can be expressed in a flowchart, see Figure 2, where the individual tasks are:

- Structural (exposure) characterisation – Defining the geometry of the structure, including uncertainties in material properties.
- Hazard analysis – Develop joint probability distribution for environmental conditions, includes wind and wave conditions in an OWF.
- Fragility analysis – Captures uncertainty in mathematical models used to estimate structural capacity and express the probability of damage occurring conditioned on the load intensity.
- Loss analysis – Probabilistic estimate of financial loss, which provides information for deciding whether or not system has sufficient capacity.

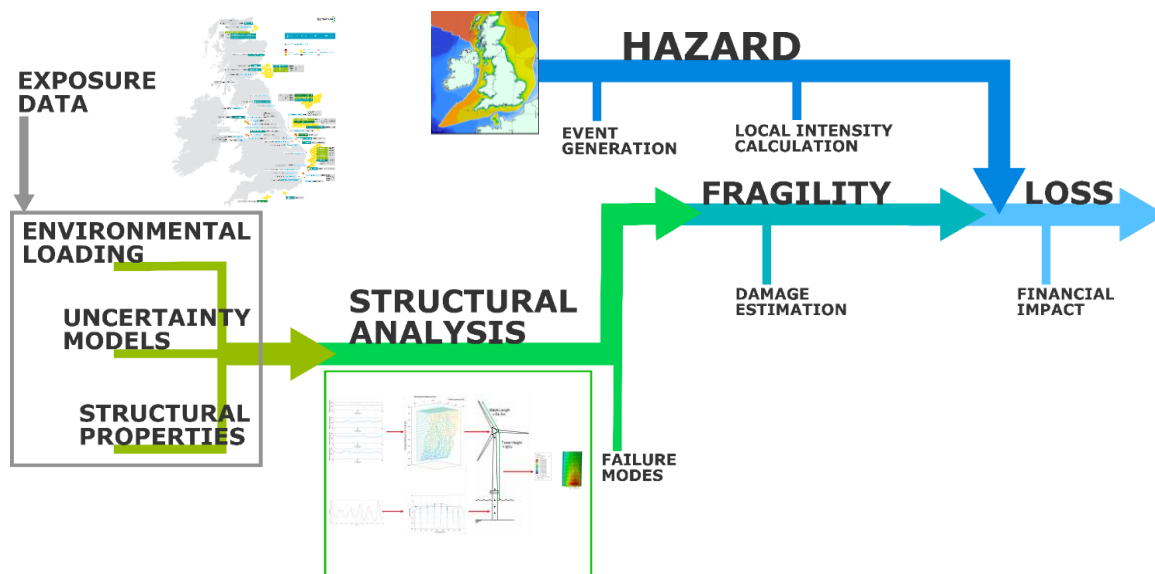


FIGURE 2. PBE framework for a single OWT structure.

The fully probabilistic formulation indicated by Equation (2) can be simplified by assuming that some of the parameters or models are deterministic, therefore reducing the order of the integration. Specifically, this paper assumes that the damage-to-cost value is constant (all towers are assumed to have the same material cost) for a single limit state corresponding to local failure of the structural components (tower and monopile). Where failure in the ultimate limit state (ULS) is evaluated using deterministic code provisions [13]. Based on these assumptions, the probability of failure required for the full loss calculation can be calculated using only the fragility and hazard components shown on Figure 2, as is shown later in Section 3.3.

2.2 System Failure

The wind turbine is modelled as a system comprised of mechanical and structural components. In the general case, a system with independent components (N), each of which has discrete failure states, will have a finite number of system failure conditions, i.e. combinations of all the component failure states. These combinations can be summarised in a matrix K [17] where each individual component has two states, either: functioning or failure, where a value of 1 is used to indicate that the component fails and 0 to indicate that the component remains is operational. The matrix will have entries $k_{ij} \in \mathbb{Z}^{N \cdot 2^N}$; for the 12 OWT components listed on Table 3, the matrix will have entries $k_{ij} \in \mathbb{Z}^{12 \cdot 4096}$, where the first column will read $[0 \ 0 \ 0 \ 0 \ 0 \ 0 \ 0 \ 0 \ 0 \ 0 \ 0 \ 0]^T$ indicating the case in which all components are functional, and the last $[1 \ 1 \ 1 \ 1 \ 1 \ 1 \ 1 \ 1 \ 1 \ 1 \ 1 \ 1]^T$ indicating the case where all components have failed. The intermediate columns contain all possible permutations of 1s and 0s indicating different partial failure states.

If each component has a deterministic material replacement cost, the discrete system failure events can be combined to assess the probability of incurring a repair cost (c_r). The matrix of the failure events K is converted into a failure cost matrix K_c by multiplying each column of K by a vector containing the failure cost of each component. This new matrix will contain the same number of elements as K but the values will equal to the failure cost of each component as opposed to a logical (1 or 0). Then $P_{sys}(c_r)$ can be defined as the probability that a set of components fail $k^* \in K_c$ whose combined repair cost is equal to the target (c_r):

$$P_{sys}(c_r) = \sum_{k^* \in K_c} \prod_{i=1}^N P_i^{k_i} (1 - P_i)^{1-k_i} \quad (3)$$

$P_{sys}(c_r)$ is summed over all the columns of the K matrix where the total repair cost of the components equals c_r , i.e. k^* is a subset of K containing all equal cost vectors of system status. The probability of each total material cost is the product of the individual component failure probabilities in the matrix of failure events K as this calculation assumes each component is independent. When k_i is 0 then the probability that the component survives is used $(1 - P_i)^{1-k_i}$ and if k_i is 1 then the probability that the component fails is used $P_i^{k_i}$. The result is the combined probability that a set of conditions (defined by k^*) will occur.

3 CASE STUDY EXAMPLE – STRUCTURAL FRAGILITY

An example is used to illustrate applying the loss calculation framework, described in Section 2, to the site of a real-world offshore wind farm. Here resilience is estimated using consequence of failure alone, in the form of financial material costs. The procedure described in Section 2 is implemented in two steps: firstly, fragility curves are defined for a representative, index turbine and, secondly, the loss calculation is performed, using the fragility curves combined with empirically derived equipment failure data. This section describes the fragility calculation for an OWT structural components.

3.1 Site Selection and Structural Model

Environmental conditions for the Kriegers Flak OWF site [18] are shown on Figure 3 (right), where mean wind speeds and significant wave heights are plotted against their corresponding mean return period (MRP). The water depth of this is around 20m, making it a suitable location for the NREL 5MW OWT on a monopile foundation, as shown on Figure 3 (left) which has a 30m long and 6m diameter monopile. As indicated on the figure the tower terminates at an elevation above mean sea level of 87.7m. A full list of dimensions and material properties of the turbine are provided by Jonkman et al [19].

The probability of incurring different repair costs was estimated using the calculation described in Section 4.1. The component failure rates for individual turbines were scaled to a farm by multiplying them by the number of turbines, assumed a medium sized wind farm with 80 individual OWT (for comparison Rampion has 116 and London Array 175 turbines [20]).

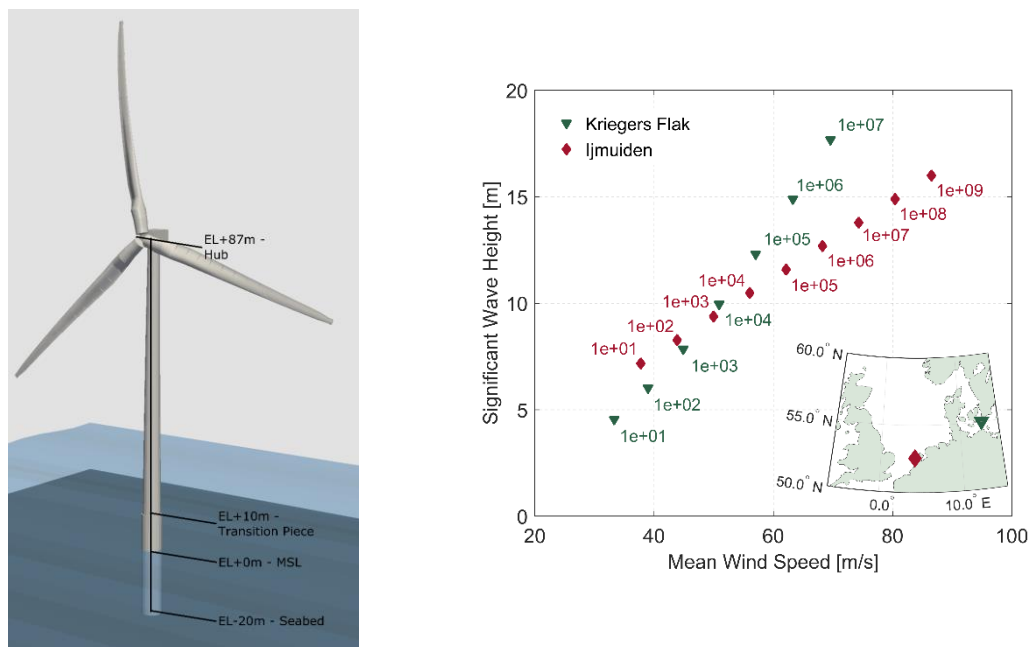


FIGURE 3. Image of the OWT structural model in FAST, with main elevations highlighted (left). Comparison of the extreme wind and wave conditions associated with different MRP at Kriegers Flak [18] and Ijmuiden [21] OWF sites (right), inset map shows the locations of both sites.

3.2 Fragility Curves

Fragility curves were developed for the NREL 5MW OWT located at the Kriegers Flak site using MRP as IM parameter by the authors [13] by selecting 16 MRP (as indicated on Table 1) and calculating the probability of failure. At each 400 structural simulations were run where the only statistical variability between the 400 simulation runs is a result of the stochastic wind and wave loading.

A one or zero was assigned to each analysis depending on whether the tower or monopile was predicted to fail during the simulation. The probability of failure was taken to be the mean of this index over all 400 samples, for example a probability of failure of 0.5 is just the average of a vector comprised of 200 ones and 200 zeros. Error in the probability of failure prediction was predicted by assuming that the scatter in probability of failure follows a binomial

distribution [22], which is suitable as each analysis is assumed independent, the probability mass function (PMF) shown in Equation (4):

$$P(x = k) = \binom{n}{k} \cdot p^k \cdot (1 - p)^{n-k} \quad (4)$$

Where n is the sample size, p is the probability of failure calculated by taking the mean of the indicator variables and k is the number of observed failure samples. Based on Equation (4) the variability in prediction of the probability of failure will hold a maximum value when the probability of failure is 0.5 and will be 0 when the probability of failure is either 0 or 1, as the standard deviation will be 0 at these points.

The data on Table 1 was used to fit a fragility curve, which provided a continuous prediction of probability of failure, by using the maximum likelihood estimation to fit a lognormal distribution (which has the parameters log mean μ_{LN} and log standard deviation σ_{LN}). The mean value of fragility is the probability of failure calculated as described in the previous paragraphs, and the best fit lognormal distribution is described by the 'mean' parameters shown on Table 2 with the curves defined by these parameters are shown in black on Figure 4 for both structural components. The MRP in Table 1 were scaled by a factor of 100 when fitting the distribution parameters defined on Table 2 to improve the stability of the fit.

Additional post-processing was conducted to assess the error introduced by using a limited sample size on the parameters of the lognormal distribution. Monte Carlo simulation was used to sampling from each normal distribution at the 16 MRP, using the calculated mean and error as the distribution parameters. The resulting variability in lognormal curves, shown in grey lines on Figure 4, can be used to estimate the variability in the lognormal distribution parameters. This means that the fragility curves for the monopile and tower can be defined as stochastic with both the mean and standard deviation parameters as random variables, as indicated on Table 2. The normality of the lognormal distribution parameters is confirmed on Figure 5, where the four random variables are found to be approximately normally distributed with kurtosis values around 3, per the definition of a normally distribution [23].

TABLE 1. MRP with corresponding probability of failure and standard error for the monopile and tower.

MRP	Pf Monopile	Pf Tower
1.00E+02	0	0
3.00E+02	0	0
1.00E+03	0	0
3.00E+03	0	0
1.00E+04	0	0
3.00E+04	0	0.0025
1.00E+05	0	0.0125

3.00E+05	0	0.13
1.00E+06	0	0.4975
3.00E+06	0	0.8775
1.00E+07	0.005	0.9825
3.00E+07	0.0125	1
1.00E+08	0.095	1
3.00E+08	0.2425	1
1.00E+09	0.6525	1
3.00E+09	0.95	1

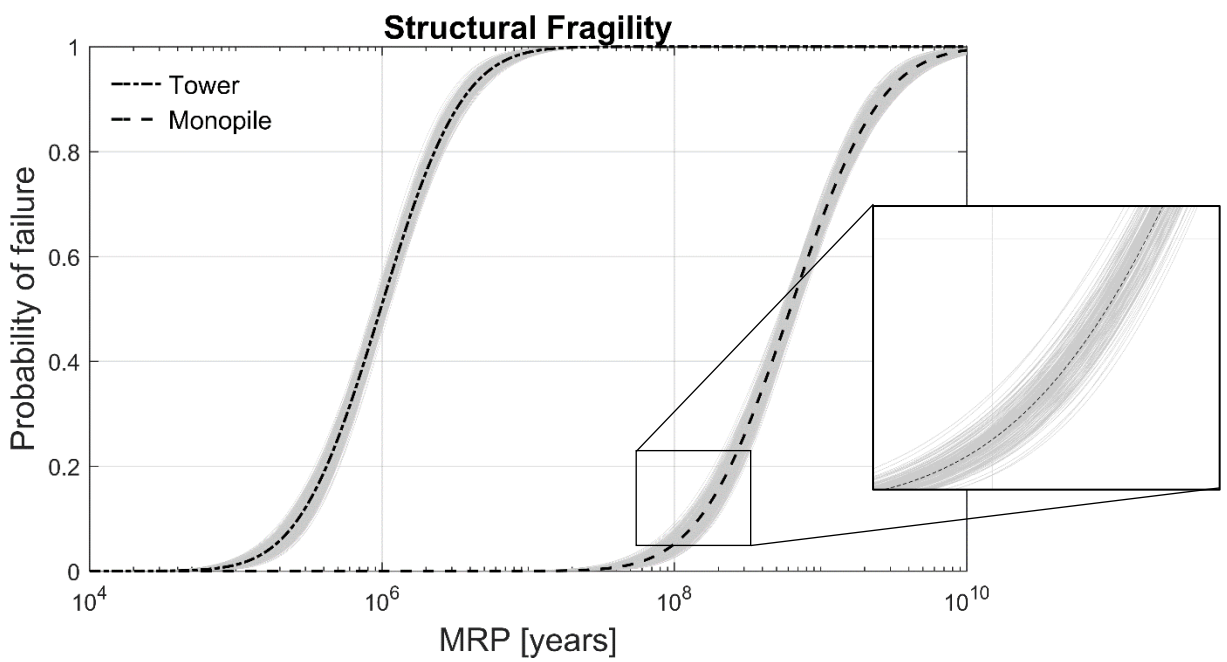


FIGURE 4. Fragility curves for the tower (left) and monopile (right). The grey lines indicate 100 Monte Carlo samples of from the normal distributions at the 16 MRP used to fit the fragility curve.

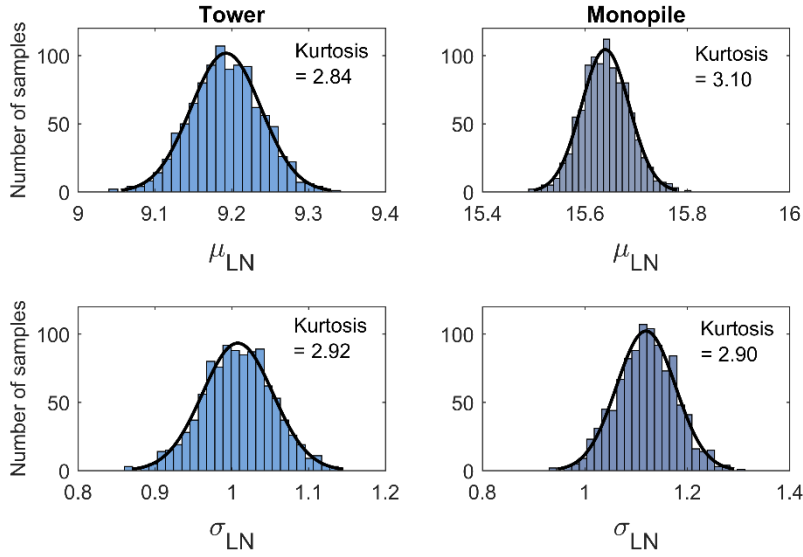


FIGURE 5. Histograms showing variability in parameters which were used to define the tower and monopile fragility curve. Based on 1000 samples of each normally distributed MRP P_f . Black lines are the best fit normal distributions.

TABLE 2. Random variables associated with the fragility curve fit parameters.

		Tower	Monopile
μ_{LN}	Mean	9.1925	15.6401
	Standard deviation	0.0456	0.0467
σ_{LN}	Mean	1.0078	1.1196
	Standard deviation	0.0458	0.0574

3.3 Structural Component Probability of Failure

As discussed previously, fragility curves represent the expected damage to a component given a level of hazard intensity (IM) and can be expressed as a conditional probability of failure ($G[DM|IM]$). However, to combine structural failure with the failure rates of the other OWT sub-systems, we need to convert the distribution into the yearly probability of failure (P_f^{Yr}) by applying the total probability theorem:

$$P_f^{Yr} = \int G[DM|IM] \cdot f(IM) \cdot dIM \approx \sum G[DM|IM] \cdot \left(\frac{1}{MRP_i} - \frac{1}{MRP_{i+1}} \right) \cdot dIM \quad (5)$$

In previous work [13] fragility curves for the tower and monopile of the NREL 5MW OWT were calculated at the Krieger's Flak OWF site, the set used in this work are shown on Figure 4. These are based on 10-minute length time-history analyses with MRP is used as the IM; which can be thought of as the inverse of an average rate of exceedance, and therefore the annual probability of occurrence can be summarised using a Binomial distribution as indicated in Equation (4). The annual probability of occurrence was calculated using numerical integration with a step size (dIM) of 20 to solve Equation (5).

The mean yearly probability of failure of an individual turbine monopile using Equation (5) is assessed to be $1.7e-7$ and the tower $1.7e-4$, also shown on Table 3, the standard deviation of

both is a factor of 5 times smaller than the mean. This indicates the variability in loss due to statistical uncertainty in the fragility curve is will be small and is therefore neglected in the following analysis.

3 CASE STUDY EXAMPLE – LOSS

4.1 Structural Failure Cost

The material cost of the two structural components was calculated independently and are indicated on Table 3, the following paragraph describes the background and assumptions.

Total offshore turbine cost (c_{WT}) in k€, including blades and drivetrain but excluding foundations, was estimated using an equation derived by fitting a relationship between turbine costs at seven different power ratings, 2MW through to 5MW, parameterised on the rated power of the turbine (P_{WT}) in MW [25]. The equation was converted into Euros by Dicorato et al [26]:

$$c_{WT} = 2.95 \cdot 10^3 \cdot \ln(P_{WT}) - 375.2 \quad (6)$$

Analysis by the National Renewable Energy Laboratory (NREL) [27] reported that cost of the tower of an onshore wind turbine comprised 17.6% of the total turbine cost. We calculate the tower for an OWT cost assuming that the relative cost of components on an onshore and OWT remains constant, using 17.6% of the value predicted from Equation (6).

The OWT foundation cost in k€ (c_{FN}) was estimated using a parametric equation [26]:

$$c_{FN} = 320 \cdot P_{WT} \cdot (1 + 0.02(D - 8)) \cdot (1 + 8 \cdot 10^{-7}(h(0.5d)^2 - 10^5)) \quad (7)$$

Where the cost estimate depends on: D the water depth (m), h the hub height above mean sea level (m) and d the rotor diameter (m). The equation originated from a 2003 feasibility study into OWT, and was validated against actual foundation costs from five real OWF. The average error was large, at 8.7%, but Equation (7) was found to predict foundation cost better than two other models derived using fewer parameters [26].

4.2 Equipment Failure Rates and Cost

Failure data for the non-structural components of the OWT were taken from the work of Carroll et al [12]. They analysed data from maintenance records of ~350 OWT ranging from 2MW to 4MW and presented the results for different sub-systems, details of the portfolio are not clear as commercial sensitivity means the data was anonymised. Only the failure rates and material costs relating to the top 10 sub-systems in terms of major replacement cost (out of a total of 19 sub-systems) were used in this work and are shown on Table 3. Additionally, costs were rounded to the nearest €1000, to improve computational efficiency when evaluating Equation (3).

TABLE 3. Material cost for major replacement of OWT sub-assemblies.

¹Equation (6) with data – [$P_{WT} = 5MW$]. ²Equation (7) with data – [$D = 20m$; $h = 87.6m$; $d = 126m$].

Source	Component	Major replacement [€]	Failure rate [/turbine/year]
Carroll [12]	Gearbox	230,000	0.154
	Hub	95,000	0.001
	Blades	90,000	0.001
	Transformer	70,000	0.001
	Generator	60,000	0.095
	Circuit breaker	14,000	0.002
	Power supply	13,000	0.005
	Pitch system	14,000	0.001
	Yaw system	13,000	0.001
	Controller	13,000	0.001
Parametric equations	Tower	770,000 ¹	$1.70 \cdot 10^{-4}$
	Monopile	2,380,000 ²	$1.70 \cdot 10^{-7}$
Total Cost		3,762,000	

4.3 Combined Loss Assessment

The loss estimation was computed using the mean parameters for the fragility curve described in Table 1, therefore the fragility curve has no uncertainty associated prediction of the probability of failure. Three loss calculations are compared:

1. Equipment only, using just empirical data,
2. Structural and equipment components, where all are independent,
3. Structural and equipment components, where failure of the tower causes all equipment to fail and failure of the monopile causes all equipment and the tower to fail too.

The resulting loss profile is shown on Figure 6. Low repair cost failures occur with relatively large probability and these are driven by the more frequently occurring equipment failures, see profile is approximately the same shape for all methods. However, the PMF which excludes structural failures cannot predict repair costs above 1M€ all of which include the tower or monopile. The PMF with independent components predicts a range of failure modes involving the tower, whereas the PMF with combined failure modes only predicts a higher probability larger repair cost. This is more accurate as any failure involving the tower will likely have consequences for all equipment in the hub. The very high repair cost failure at 3,762,000€, which is driven by failure of the monopile in conjunction with other components is not visible due to their rarity, correlated annual failure probability is $1.331e-5$. This low occurrence is a result of the MRP at which the monopile begins to fail from the fragility curve, see Figure 4.

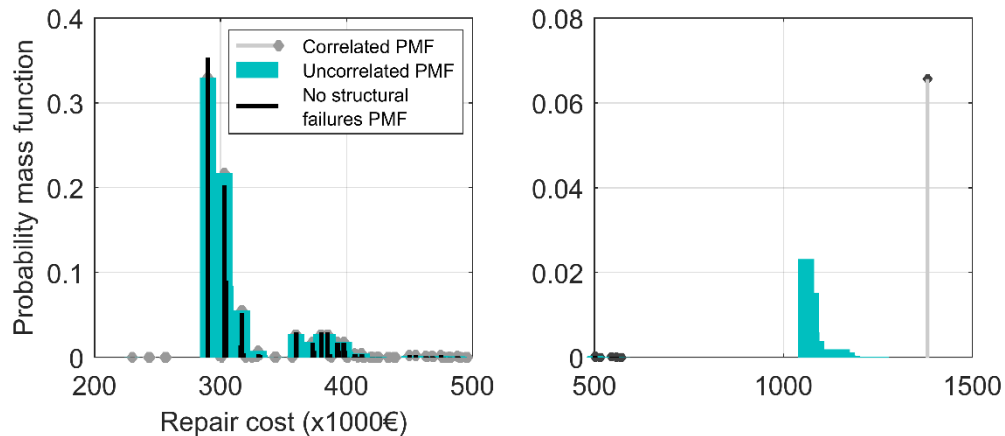


FIGURE 6. Loss PMF using three calculated using 3 assumptions: only equipment (thin black line), equipment and structure where all components are independent (cyan), and equipment and structure where the failure of the structure results in failure of all other equipment (grey).

4 CONCLUSION

The developing concept of resilience provides an alternative approach, which may allow us to consider performance of OWF as a whole. This paper proposes a framework for estimating resilience of OWF by applying the existing framework of PBE. A case study demonstrates how this calculation may be implemented to estimate potential loss associated with the multiple sub-systems present on individual turbines at the OWF level.

In this study, structural resilience is simplified to estimation of the consequence of the turbines failure, which is defined in terms of material cost alone. This allows the idea of resilience to be applied by practicing engineers who will not have access to data required for a full evaluation of resilience, including potential recovery phases. As robustness is a component of a full resilience calculation, the simplified method presented in this paper could be used as an input to a more comprehensive resilience assessment.

The case study presented included both generation equipment and structural. Although structural failure was found to be rare it was associated with very high material costs, which are relevant when considering the overall vulnerability of a wind farm that is comprised of many individual turbines. Additionally, the structure will be site specific, therefore need to include details of site loading into risk calculation, fragility will vary between sites [13].

Future steps will involve considering the risk posed to an array or whole OWF in greater detail, due to correlated hazards i.e. a wind storm effects the whole installation simultaneously. Many challenges remain to be answered, particularly relating to the choice of performance indicators [13]. However, if successful, this approach will aid in the development of integrated design techniques for OWF and therefore works towards meeting the goals set by the UK government cost reduction framework for offshore wind.

ACKNOWLEDGEMENTS

This work was supported by the UK Engineering and Physical Sciences Research Council (EPSRC), DTP grant EP/M507970/1 for University College London.

REFERENCES

- [1] "The European offshore wind industry - key trends and statistics 2015," 2016.
- [2] A. Ho and A. Mbistrova, "The European offshore wind industry - key trends and statistics 1st half 2016," 2016.
- [3] "Wind in power - 2015 European statistics," 2016.
- [4] P. Arwas and D. Charlesworth, "Offshore wind cost reduction: pathways study," 2012.
- [5] J. Van Der Tempel, "Design of support structures for offshore wind turbines," Technical University of Delft, 2006.
- [6] International Electrotechnical Commission, *IEC 61400-3. Wind turbines - Part 3: design requirements for offshore wind turbines*. 2009.
- [7] DNV GL, *DNVGL-ST-0126. Support structures for wind turbines*. 2016, p. 182.
- [8] M. Bruneau, M. Eeri, S. E. Chang, M. Eeri, T. Ronald, M. Eeri, G. C. Lee, M. Eeri, T. D. O. Rourke, M. Eeri, A. M. Reinhorn, M. Eeri, M. Shinozuka, M. Eeri, W. A. Wallace, and D. Von Winterfeldt, "A framework to quantitatively assess and enhance the seismic resilience of communities," vol. 19, no. 4, pp. 733–752, 2003.
- [9] M. Ghosn, M. Asce, L. Due, M. Shah, F. Asce, M. Akiyama, M. Asce, F. Biondini, M. Asce, S. Hernandez, and M. Asce, "Performance indicators for structural systems and infrastructure networks," vol. 142, no. 9, pp. 1–18, 2016.
- [10] M. Bruneau and A. Reinhorn, "Exploring the concept of seismic resilience for acute care facilities," *Earthq. Spectra*, vol. 23, no. 1, pp. 41–62, 2007.
- [11] S. E. Quiel, S. M. Marjanishvili, and B. P. Katz, "Performance-based framework for quantifying structural resilience to blast-induced damage," *J. Struct. Eng.*, vol. 142, no. 8, p. C4015004, 2015.
- [12] J. Carroll, A. McDonald, and D. McMillan, "Failure rate, repair time and unscheduled O&M cost analysis of offshore wind turbines," *Wind Energy*, vol. 19, no. 6, pp. 1107–1119, Jun. 2016.
- [13] D. Wilkie and C. Galasso, "Ultimate limit state fragility of offshore wind turbines on monopile foundations," in *Proceedings of the 12th International Conference on Structural Safety and Reliability (ICOSSAR 2017)*, 2017, pp. 174–184.
- [14] K. A. Porter, "An overview of PEER's performance-based earthquake engineering methodology," *9th Int. Conf. Appl. Stat. Probab. Civ. Eng.*, vol. 273, no. 1995, pp. 973–980, 2003.
- [15] F. Petrini, "A probabilistic approach to performance-based wind engineering (PBWE)," Università degli Studi di Roma, 2009.
- [16] M. Barbato, F. Petrini, V. U. Unnikrishnan, and M. Ciampoli, "Performance-based hurricane engineering (PBHE) framework," *Struct. Saf.*, vol. 45, pp. 24–35, 2013.
- [17] A. F. Mensah and L. Dueñas-Osorio, "A closed-form technique for the reliability and risk assessment of wind turbine systems," *Energies*, vol. 5, no. 6, pp. 1734–1750, 2012.
- [18] Niras A/S, "Kriegers Flak - metocean report," 2014.
- [19] J. Jonkman, S. Butterfield, W. Musial, and G. Scott, "Definition of a 5-MW reference wind turbine for offshore system development," 2009.
- [20] "Offshore Wind Projects Offshore Wind Project Timelines 2015," 2015.
- [21] T. Fischer, W. de Vries, and B. Schmidt, "Upwind design basis - WP4," 2010.
- [22] I. Iervolino, "Assessing uncertainty in estimation of seismic response for PBEE," *Earthq. Eng. Struct. Dyn.*, vol. 46, no. February, pp. 1711–1723, 2017.
- [23] J. Benjamin and C. Cornell, *Probabality, statistics and decision for civil engineers*. New York: McGraw-Hill, 1970.
- [24] J. D. Sorensen and H. S. Toft, "Probabilistic design of wind turbines," *Energies*, vol. 3, no. 2, pp. 241–257, 2010.
- [25] "Study of the costs of offshore wind generation: a report to the renewables advisory board & DTI," 2007.
- [26] M. Dicorato, G. Forte, M. Pisani, and M. Trovato, "Guidelines for assessment of investment cost for offshore wind generation," *Renew. Energy*, vol. 36, no. 8, pp. 2043–2051, 2011.
- [27] C. Mone and B. Maples, "2013 cost of wind energy review - NREL/TP-5000-63267," 2015.